Supplementary information

Genetic evidence suggests that Spata22 is required for the maintenance of Rad51 foci in mammalian meiosis

Satoshi Ishishita[1], Yoichi Matsuda[2] & Kazuhiro Kitada[3]

[1]Division of Bioscience, Graduate School of Environmental Earth Science, Hokkaido University, North 10 West 8, Kita-ku, Sapporo 060-0810, Japan, [2]Laboratory of Animal Genetics, Graduate School of Bioagricultural Sciences, Nagoya University, Furo-cho, Chikusa-ku, Nagoya, Aichi 464-8601, Japan, [3]Division of Bioscience, Graduate School of Science, Hokkaido University, North 10 West 8, Kita-ku, Sapporo 060-0810, Japan

Supplementary Methods

Immunohistochemistry. Testes were collected from each of the two wild-type males and *tm* homozygous mutant males at three months after birth. They were fixed using 10% neutral buffered formalin, dehydrated, embedded in paraffin, and then cut to 5 μm thickness. Immunostaining was conducted using a polyclonal rabbit Spata22 antibody. The primary antibody was used at 1:100 dilution and incubated at 4°C for 24 h. Staining was developed using the Vectastain ABC kit (Vector) in accordance with the manufacturer's standard protocol.

Supplementary Table 1.
The number of Rad51, Spata22, and Mlh1 foci during each substage of prophase I.

Stage	Number of foci per nucleus (mean ± s.d.)					
	Rad51		Spata22		Mlh1	
Early leptotene	10.9 ± 5.4	(*n* = 7)	ND	(*n* = 10)	NE	
Leptotene	72.7 ± 25.6	(*n* = 7)	45.0 ± 19.6	(*n* = 5)	NE	
Early zygotene	160.8 ± 50.6	(*n* = 16)	211.1 ± 59.9	(*n* = 11)	NE	
Mid-zygotene	161.9 ± 28.6	(*n* = 8)	305.9 ± 15.3	(*n* = 12)	NE	
Late zygotene	125.7 ± 21.9	(*n* = 7)	238.2 ± 31.1	(*n* = 10)	NE	
Early pachytene	31.3 ± 10.1	(*n* = 6)	202.7 ± 21.1	(*n* = 6)	11.4 ± 6.5	(*n* = 13)
Mid-pachytene	24.4 ± 11.4	(*n* = 8)	139.1 ± 18.3	(*n* = 8)	20.9 ± 2.7	(*n* = 9)
Late pachytene	ND	(*n* = 6)	20.1 ± 12.3	(*n* = 7)	15.8 ± 3.0	(*n* = 12)
Diplotene	NE		ND	(*n* = 5)	10.7 ± 6.7	(*n* = 3)

s.d., standard deviation; *n,* number of nuclei; ND, not detected; NE, not examined.

Supplementary Table 2.
Quantification of colocalisation of Spata22 and Rpa proteins in spermatocyte nuclei.

Stage	Number of foci/nucleus (mean ± s.d.)			Percentage (mean ± s.d.)				
	Spata22	Spata22 & Rpa	Rpa	Spata22 only	Spata22 & Rpa	Rpa only	Spata22 & Rpa in Spata22	Spata22 & Rpa in Rpa
Leptotene-like (*n* = 5)	54.0 ± 18.6	40.6 ± 11.0	55.2 ± 12.9	17.1 ± 12.5	60.3 ± 8.3	22.6 ± 5.7	78.6 ± 15.0	72.9 ± 3.7
Zygotene-like (*n* = 5)	385.2 ± 29.9	379.8 ± 31.9	387.4 ± 30.7	1.4 ± 1.2	96.7 ± 2.6	1.9 ± 1.4	98.6 ± 1.3	98.0 ± 1.4
Pachytene-like (*n* = 5)	191.6 ± 36.4	189.2 ± 36.5	195.8 ± 34.8	1.2 ± 0.7	95.2 ± 1.7	3.5 ± 1.5	98.7 ± 0.8	96.4 ± 1.5

s.d., standard deviation; *n,* number of nuclei.

Supplementary Table 3.

Quantification of colocalisation of Spata22 and Rad51 proteins in spermatocyte nuclei.

Stage	Number of foci/nucleus (mean ± s.d.)			Percentage (mean ± s.d.)				
	Spata22	Spata22 & Rad51	Rad51	Spata22 only	Spata22 & Rad51	Rad51 only	Spata22 & Rad51 In Spata22	Spata22 & Rad51 in Rad51
Leptotene-zygotene-like (*n* = 5)	177.8 ± 35.2	115.8 ± 30.5	256.2 ± 29.8	19.6 ± 7.0	36.2 ± 8.2	44.2 ± 9.9	65.1 ± 10.4	45.2 ± 10.3
Zygotene-like (*n* = 5)	282.6 ± 20.8	123.2 ± 27.0	236 ± 40.8	40.6 ± 5.7	31.0 ± 4.9	28.4 ± 3.4	43.4 ± 7.0	52.1 ± 5.1
Early-mid-pachytene-like (*n* = 5)	156.6 ± 13.7	54.6 ± 13.4	82.0± 22.0	55.5 ± 9.6	30.4 ± 10	14.1 ± 8.2	35.2 ± 10.3	68.6 ± 15.1

s.d., standard deviation; *n,* number of nuclei.

Supplementary Table 4.

Quantification of colocalisation of Spata22 and Mlh1 proteins in spermatocyte nuclei.

Stage	Number of foci/nucleus (mean ± s.d.)			Percentage (mean ± s.d.)				
	Spata22	Mlh1 & Spata22	Mlh1	Spata22 only	Spata22 & Mlh1	Mlh1 only	Spata22 & Mlh1 in Spata22	Spata22 & Mlh1 in Mlh1
Early-mid-pachytene-like (*n* = 5)	125.4 ± 23.4	14.8 ± 1.5	17.6 ± 2.4	85.8 ± 3.9	11.9 ± 2.8	2.3 ± 1.7	12.2 ± 2.9	84.7 ± 7.5
Late pachytene-like (*n* = 5)	30.8 ± 7.8	2.6 ± 2.2	26.6 ± 3.5	50.9 ± 5.1	4.8 ± 3.6	44.3 ± 4.9	8.4 ± 6.3	9.8 ± 7.3

s.d., standard deviation; *n,* number of nuclei.

Supplementary Table 5.
The number of Rpa and Rad51 foci in wild-type and *tm/tm* spermatocytes.

Stage	Number of foci/nucleus (mean ± s.d.)			
	Rpa		Rad51	
	Wild type	*tm/tm*	Wild type	*tm/tm*
Early leptotene (WT) Early leptotene-like (*tm/tm*)	ND (n = 6)	ND (n = 5)	13.6 ± 7.1 (n = 8)	14.9 ± 7.8 (n = 9)
Leptotene (WT) Leptotene-like (*tm/tm*)	35.7 ± 22.2 (n = 7)	40.5 ± 19.1 (n = 12)	72.4 ± 19.5 (n = 13)	58.5 ± 11.8* (n = 10)
Early zygotene (WT) Early zygotene-like (*tm/tm*)	171.7 ± 52.7 (n = 27)	156.4 ± 68.7 (n = 23)	158.0 ± 50.3 (n = 29)	60.9 ± 23.1** (n = 35)
Mid-zygotene (WT) Mid-late zygotene-like (*tm/tm*)	293.2 ± 36.1 (n = 9)	306.5 ± 22.8 (n = 22)	161.9 ± 28.6 (n = 8)	9.9 ± 8.8** (n = 28)
Late zygotene (WT) Mid-late zygotene-like (*tm/tm*)	221.6 ± 21.0 (n = 9)	306.5 ± 22.8** (n = 22)	132.8 ± 26.3 (n = 12)	9.9 ± 8.8** (n = 28)

s.d., standard deviation; *n,* number of nuclei used for examination; ND, not detected; ** and *, statistically significant with the wild type at 1 and 5% probability by the Mann–Whitney U-test (two-tailed).

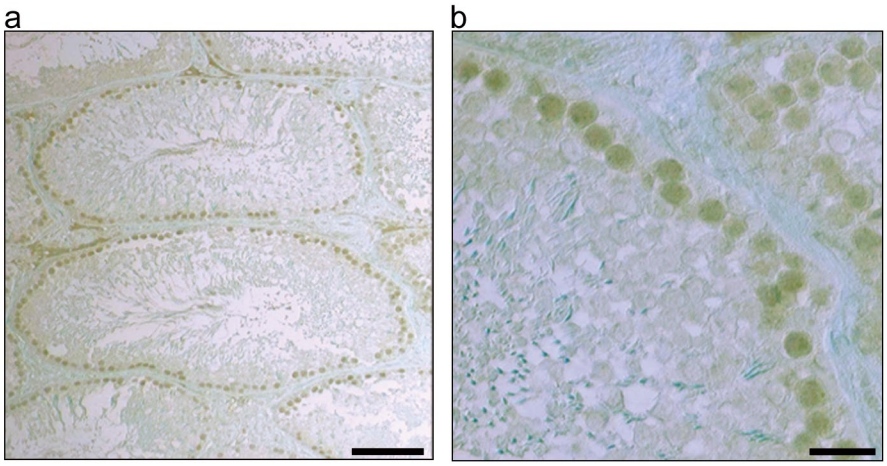

Supplementary Figure 1. Spata22 is expressed in the nuclei of rat primary spermatocytes. (**a**, **b**) Immunohistochemistry of the adult wild-type testis with anti-Spata22 antibody. Spata22 expression was restricted to the spermatocytes (**a**, dark brown staining). Higher magnification shows discrete subnuclear staining in spermatocytes (**b**). Nuclei were counterstained with methyl green.

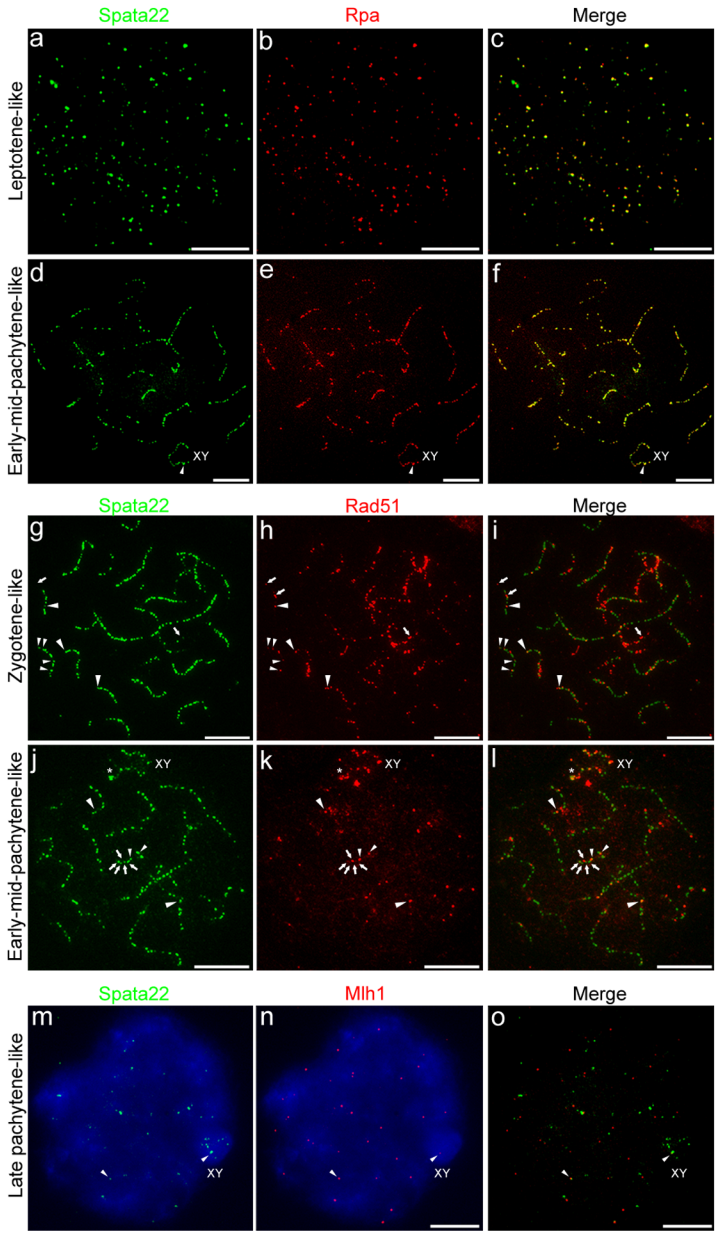

Supplementary Figure 2. Colocalisation of Spata22 with Rpa, Rad51, and Mlh1 in spermatocyte nuclei. (**a**–**f**) Immunolocalisation of Spata22 (green) and Rpa (red) in the spermatocyte nuclei at the leptotene-like (**a**–**c**) and early-mid-pachytene-like (**d**–**f**) stages. Spata22 and Rpa foci overlapped extensively with each other in both substages. Colocalisation of the two proteins was found in the terminal segments of sex chromosomes in the early-mid-pachytene-like nucleus (**d**–**f**, arrowheads). (**g**–**l**) Immunolocalisation of Spata22 (green) and Rad51 (red) in the nuclei at the zygotene-like (**g**–**i**) and early-mid-pachytene-like (**j**–**l**) stages shows that a subset of the Spata22 foci overlapped with Rad51 foci. Complete overlap, partial overlap, and non-overlap between the two proteins' foci are indicated by large arrowheads, small arrowheads, and arrows, respectively (**g**–**l**). Mixed foci were present in the sex chromosomes (XY) in the early-mid-pachytene-like nucleus (**j**–**l**, asterisks). (**m**–**o**) Immunolocalisation of Spata22 (green) and Mlh1 (red) in the late pachytene-like nucleus. The nucleus was counterstained with 4',6-diamidino-2-phenylindole (DAPI) (blue). Mlh1 foci and Spata22 foci overlapped with each other at two sites in the nucleus (arrows). Scale bars in all panels, 10 μm.

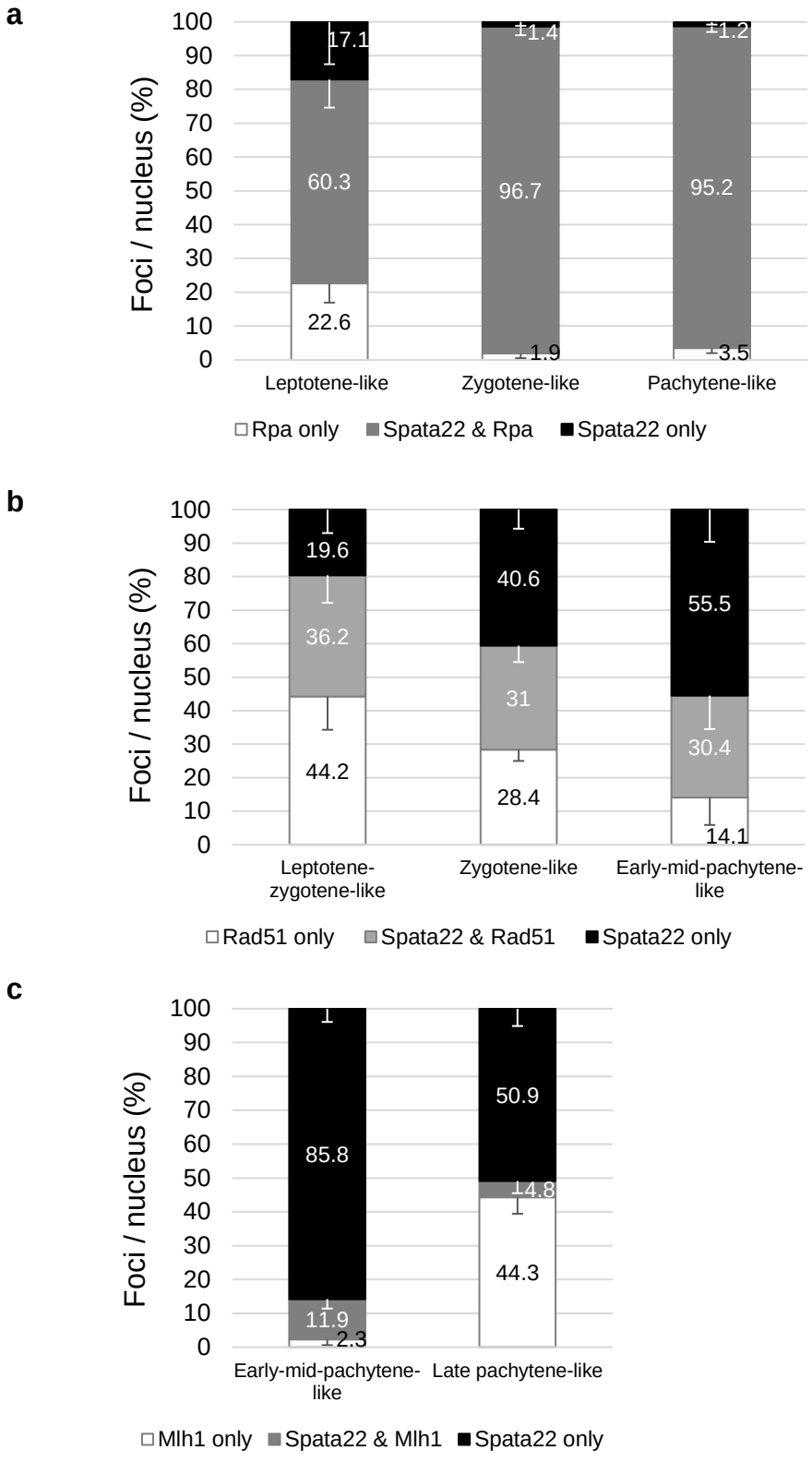

Supplementary Figure 3. Quantification of coexistence of Spata22 and Rpa (a), Rad51 (b), or Mlh1 (c) in spermatocyte nuclei. For each stage, non-overlapping foci of each protein and pairs of overlapping proteins' foci were counted per nucleus. The percentage of non-overlapping foci or overlapping focus pairs was determined. Numerical values represent the mean; the bars denote standard deviation. Five nuclei were analysed per stage.

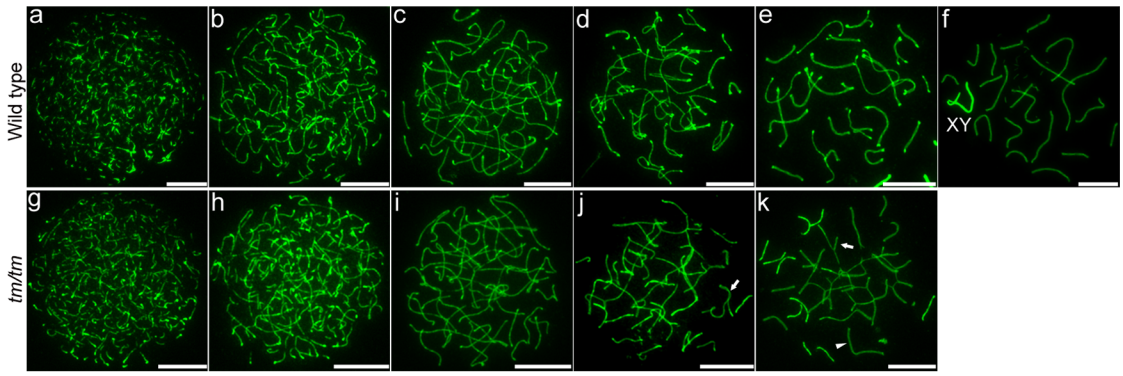

Supplementary Figure 4. Meiotic progression in the *tm* homozygous rat.

(**a**–**k**) Immunolocalisation of Sycp3 (green) in the spread nuclei of the wild-type (upper panels) and *tm* homozygous (lower panels) spermatocytes at the leptotene (**a**), early zygotene (**b**, **c**), mid-zygotene (**d**), late zygotene (**e**), pachytene (**f**), leptotene-like (**g**), early zygotene-like (**h**, **i**), and mid-late zygotene-like (**j**, **k**) stages. Chromosome morphologies were normal in the mutant nuclei during the leptotene- and early zygotene-like stages (**a**–**c**, **g**–**i**). Representatives of mutant nuclei at the mid-late zygotene-like stage that contain chromosomes that exhibit non-homologous pairing (arrows) (**j**, **k**). Representative of mutant nucleus at the mid-late zygotene like stage that contains chromosomes that exhibit homologous pairing (arrowhead) (**k**). The representative of wild-type nucleus at pachytene that shows completion of homologous chromosome pairing (**f**). “XY” indicates the sex chromosomes. Scale bars in all panels, 10 μm.

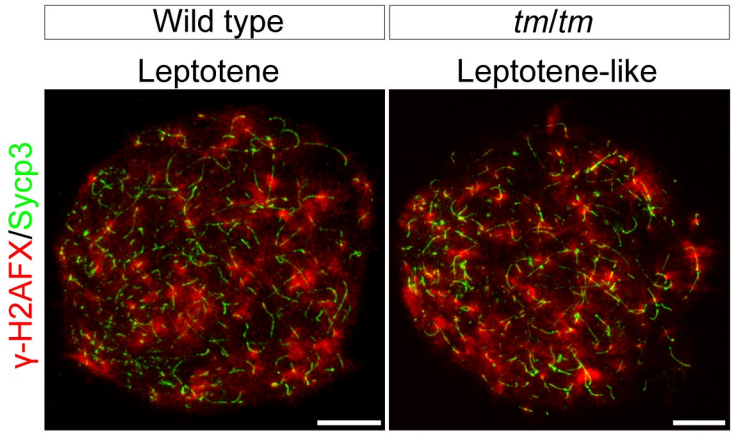

Supplementary Figure 5. Distribution of γ-H2AFX in the wild-type leptotene and *tm* homozygous leptotene-like spermatocytes. Immunolocalisation of γ-H2AFX (red) and Sycp3 (green) in the wild-type (left) and *tm* homozygous (right) spermatocyte nuclei. γ-H2AFX was distributed throughout the chromatin in both the wild-type leptotene and mutant leptotene-like spermatocytes. Scale bars in all panels, 10 μm.

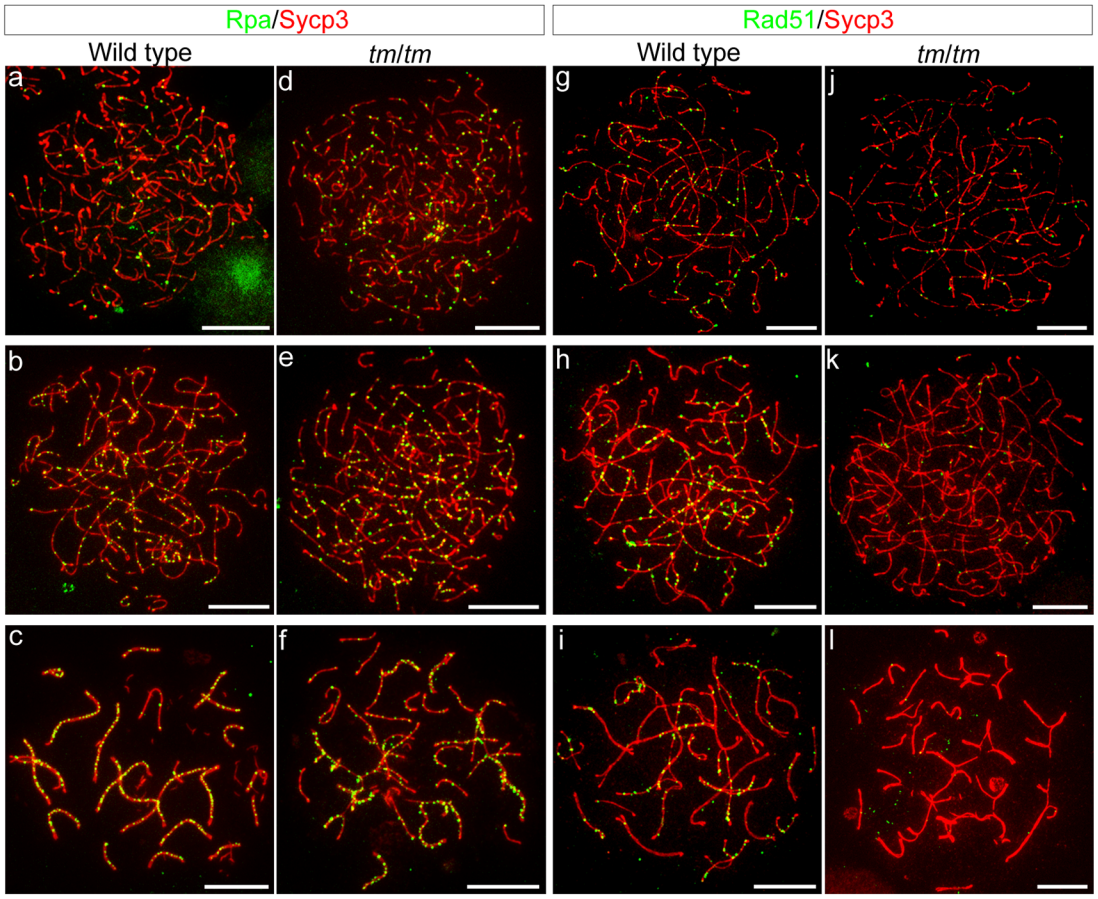

Supplementary Figure 6. Effects of *Spata22* deletion on localisations of Rpa and Rad51. (**a**–**f**) Immunolocalisation of Rpa (green) and Sycp3 (red) in the wild-type (left panels) and *tm* homozygous (right panels) spermatocyte nuclei at the early zygotene (**a**, **b**), late zygotene (**c**), early zygotene-like (**d**, **e**), and mid-late zygotene-like (**f**) stages. Rpa foci were abundant in the mutant mid-late-zygotene-like nucleus (see **Fig. 2i**). (**g**–**l**) Immunolocalisation of Rad51 (green) and Sycp3 (red) in the wild-type (left panels) and *tm* homozygous (right panels) spermatocyte nuclei at the early zygotene (**g**, **h**), late zygotene (**i**), early zygotene-like (**j**, **k**), and mid-late zygotene-like (**l**) stages. Fewer Rad51 foci were observed in the mutant nuclei than in the wild-type controls (see **Fig. 2j**). Scale bars in all panels, 10 μm.